

POINT PROCESSES OF SEGMENTS AND RECTANGLES FOR BUILDING EXTRACTION FROM DIGITAL ELEVATION MODELS

Mathias Ortner, Xavier Descombes and Josiane Zerubia

ARIANA Research Group, INRIA/I3S,
BP 93, 06902 Sophia-Antipolis Cedex France.
Email : Firstname.Lastname@sophia.inria.fr

ABSTRACT

In this work, we propose a new model based on stochastic geometry for extracting features from images. This type of model allows the incorporation of a prior knowledge on the interactions between features within the extraction process. We focus on the specific problem of automatic building extraction from Digital Elevation Models (DEMs). The model we propose is based on two interacting spatial point processes, the former being a process of rectangles, the latter a process of segments. An energy associated with the resulting process is defined. This energy consists in five main parts. We first define two energy data terms to make the rectangles fit the homogeneous areas and the segments fit meaningful discontinuities. Two prior terms favoring respectively the alignment of rectangles and the connection of segments are incorporated. The last part of the energy is an interaction term that makes the two types of objects cooperate. We present results on real data provided by the IGN (French Geographic Institute).

1. INTRODUCTION

The automatic reconstruction of precise 3D maps of towns is an important but still open issue and remotely sensed high resolution data seem to be the natural type of data to employ for automatic urban reconstruction. However, high resolution data exhibit major issues. The preciseness of such data requires considering an image as a set of objects rather than a set of pixels. As a consequence, most of the methods developed for the automatic analysis of dense urban area are based on top-down procedures. These automatic methods are mostly made up of three steps: focus on an area of interest, low level primitive extraction and building reconstruction through primitive agglomeration. Defining automatic methods to extract relevant primitives is still an open issue. Some recent developments can be found in [1], [2] or [3]. In [4] we propose an automatic method based on stochastic geometry that proved to work well in dense urban areas. It extracts simple shapes of buildings (rectangles) from different kinds of DEMs (optical or laser). DEMs are raster data giving the altimetry of a scene: each pixel value stands for the height of the corresponding point. Such data can be obtained using stereovision techniques or laser sensors and usually exhibit a tremendous complexity.

What makes the approach we present in [4] robust to the type of data employed, is the kind of prior used. Modeling an image as a realization of a spatial point process of geometrical shapes allows

The authors would like to thank the the French Geographic Institute (IGN) for providing the images of Amiens. The first author thanks the French Defense Agency (DGA) and CNRS for partial financial support during his PhD.

the inclusion of a prior model on the patterns of features in the scene, in terms of geometrical interactions between the objects. In [4] we present a model based on rectangles. In particular, the data term consists of a discontinuity detector. In order to be able to deal with cruder data, we propose to increase the role of the spatial regularizing term. We propose to employ a method that allows the fusion of the discontinuity information with a homogeneity term. As a consequence, we consider the fusion of a process of segments together with a process of rectangles to take profit from both types of information. Note that details on the approach we present here can be found in [5].

2. SPATIAL POINT PROCESS MODELS

Let describe an image as the compact set $K = [0, X_{max}] \times [0, Y_{max}]$. An element of K is therefore a two dimensional point. A *point process* X on K is a measurable mapping from an abstract probability space $(\Omega, \mathcal{A}, \mathbb{P})$ to the set of finite configurations of points of K :

$$\forall \omega \in \Omega \quad \mathbf{X}(\omega) = \{x_1, \dots, x_n\} \quad x_i \in K.$$

A point process thereby describes random configurations of points. Point processes have been introduced in image processing by A. Baddeley and M.N.M. van Lieshout in [6] because they easily allow modeling scenes as a random set of geometrical shapes. This notion of shape is brought by the addition of marks (parameters) to each point. For instance, considering a point process on $S^r = K \times M^r$ with $M^r =]-\frac{\pi}{2}, \frac{\pi}{2}] \times [L_{min}, L_{max}] \times [l_{min}, l_{max}]$ can be seen as random configurations of rectangles since to a location in K it adds an orientation θ , a length L and a width l . Let denote \mathcal{C}^r the set of all finite configurations of rectangles. In a similar way, taking $M^s =]-\frac{\pi}{2}, \frac{\pi}{2}] \times [L'_{min}, L'_{max}]$ permits the description of random configurations of segments. Considering a point process \mathbf{X} of rectangles and a point process \mathbf{Y} of segments, we consider the following point process \mathbf{Z} on $S^r \cup S^s$:

$$\mathbf{Z}(\omega) = \mathbf{X}(\omega) \cup \mathbf{Y}(\omega).$$

What makes spatial point process models attractive for image processing applications is the possibility of defining *probability distributions* through a *probability density function*, the distribution of a reference *Poisson point process* playing the analog role of Lebesgue measure for random variables on \mathbb{R} . Let consider the distribution $\mu(\cdot)$ of a *reference Poisson point process* and a measurable mapping $h(\cdot)$ from the space of configuration of points \mathcal{C} to positive reals $[0, \infty[$ such that $Z_{norm} = \int_{\mathcal{C}} h(\mathbf{z}) d\mu(\mathbf{z}) < \infty$. Considering a point process \mathbf{Z} defined by such an unnormalized density $h(\cdot)$, and a reference measure $\mu(\cdot)$, it is possible to build a Markov chain that

converges ergodically to the distribution of \mathbf{Z} (see [7]). This sampler is incorporated within a *simulated annealing* framework which gives a global maximum of the density $h(\cdot)$ as detailed in [8]. Thus, the corresponding estimator is given by $\hat{\mathbf{z}} = \text{Argmax } h(\cdot)$ (see [5] for details).

2.1. General form of the energy

Writing the unnormalized density $h(\cdot)$ under its energetic form $U_{\mathbf{Z}}(\mathbf{z}) = -\log(h(\mathbf{z}))$, we define a model that can be decomposed as follows:

$$U_{\mathbf{Z}}(\mathbf{z}) = \rho U_{ext}(\mathbf{z}) + U_{int}(\mathbf{z}) + U_{excl}(\mathbf{z}) \quad (1)$$

$$= \rho \sum_{u \in \mathbf{z}} U_d(u) + U_{int}(\mathbf{z}) + U_{excl}(\mathbf{z}), \quad (2)$$

where $U_{int}(\mathbf{z})$ stands for an internal energy giving a spatial structure to the configuration \mathbf{z} ; $U_{ext}(\mathbf{z})$ is the external field quantifying the quality of a configuration with respect to the data and can be decomposed as a sum of energies per object $U_d(\cdot)$ while U_{excl} is an exclusion term to avoid too many superpositions of objects and is tuned such that $U(\mathbf{z} \cup u \cup u) > U(\mathbf{z} \cup u)$ for all $(u, \mathbf{z}) \in S \times \mathcal{C}$.

3. POINT PROCESS OF RECTANGLES AND BUILDINGS

We use random configurations of rectangles to describe cities. Rectangles are indeed a natural pattern to be detected in dense urban areas. We present here a model to extract rectangular homogeneous areas (full details can be obtained in [5]).

3.1. Data term

The purposes underlying the definition of the data term $U_d(\cdot)$, mapping from S to \mathbb{R} , are first to decide what an “attractive object” ($U_d(u) \leq 0$) is, and second, to introduce a potential such that minimizing $U_d(u)$ locally gives the closest attractive object.

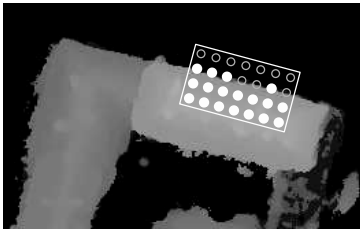


Fig. 1. The rectangle data term makes rectangles fit homogenous and extruded areas.

In order to detect rectangular homogeneous area, we use a grid of points for each rectangle (see Figure 1) and we compute different values, that describe “how homogeneous” the distribution of grey levels inside the rectangle is, and whether the inside points are higher than the outside points. In [5] we define several functions to quantify these two notions, resulting in a reward function $j_{rect} : u \rightarrow [0, 1]$ maximal for rectangles fitting well homogenous areas. We then define γ_1^r the set of rectangles $u \in S^r$ such that the inside gray levels are homogeneous enough. We call this set of rectangles the set of “attractive rectangles” and note γ_0^r the complementary set of “repulsive rectangles”. This appellation “attractive” and “repulsive” comes from the data energy term we adopt

$$U_d(u) = -j_{rect}(u) * \mathbf{1}(u \in \gamma_1^r) + 0.1 * (2 - j_{rect}(u)) \mathbf{1}(u \in \gamma_0^r),$$

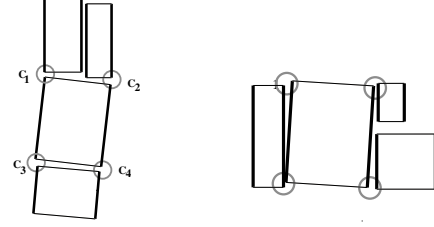


Fig. 2. Attractive interactions.

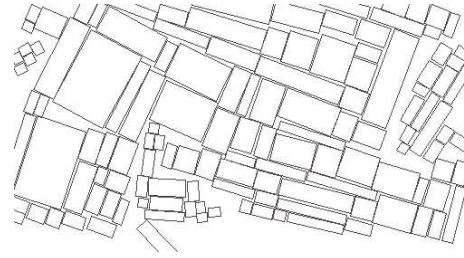


Fig. 3. Sample of the internal field of the process of rectangles.

which favors elements of γ_1^r , penalizes others and orders rectangles using the function j_{rect} .

3.2. Internal field

The prior model can be seen as a regularizing term. In our framework, the prior model is essentially composed of geometrical interactions between objects. We implemented an internal field that favors alignments between detected structures as well as a paving behavior. Details on how the internal field is defined can be found in [5]. Figure 2 presents the two types of interaction that are defined using conditions on the respective angle between two close rectangles and the distance between appropriate corners. An exclusion term that avoids redundant objects is needed to avoid redundant explanations of the data and insure that the attractive interactions do not make the set of particles collapse to an infinite accumulation of points. Furthermore, a condition used to prove the convergence of the algorithm (see [7]) requires the variation of the energy induced by adding a point to a given configuration, to be bounded. We thus use the simplest possible exclusion interaction and strongly penalize intersections between rectangles. We present on Figure 3 a sample of the process of rectangles considering only the prior term ($\rho=0$).

4. POINT PROCESS OF SEGMENTS AND DISCONTINUITIES

We introduce a point process of segments, aiming at detecting discontinuities. The general energy follows the pattern described by equation 2. Details can be found in [5].

4.1. Data term

We use the approach we introduced in [4]. As described by Figure 4, we consider for each segment some profiles and a low level filter that allows to detect significant discontinuities on each profile (see [5]). Using such a filter permits dealing with different types of data. Similarly to the case of rectangles, we define a reward function $j_{seg} : v \rightarrow [0, 1]$ that is maximal for segments fitting detected

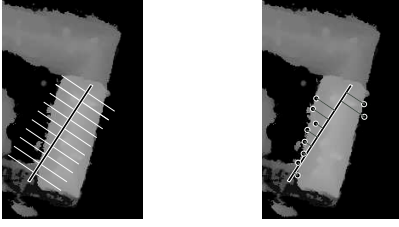


Fig. 4. The segment data term makes segments fit discontinuities detected using a set of profiles and a low level filter.

discontinuities well. We also divide the set of segments into two subsets: the set of interesting segments and its complementary (see [5]).

4.2. Internal field

The goal is to favor continuous networks. We thus introduce a connection interaction. We actually consider two kinds of connections, the first one favoring alignments between segments, the second one favoring orthogonality between them as illustrated by figure 5. The exclusion term penalizes overlapping segments. Figure 6 presents a sample of the prior term ($\rho = 0$).

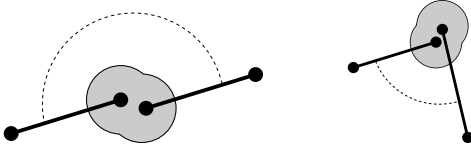


Fig. 5. Attractive interactions for segments. Left : connection in the alignment, right : connection with orthogonality

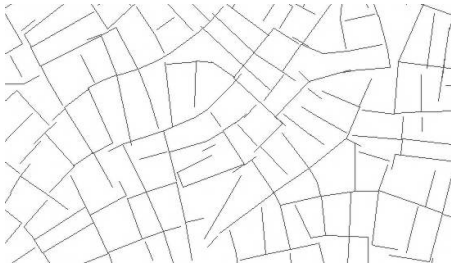


Fig. 6. Sample of the prior term acting on the process of segments

5. INTERACTION BETWEEN SEGMENTS AND RECTANGLES

We add a cooperation term between segments and rectangles. We define the following energy associated to the process Z , which consists of a superposition of segments and rectangles:

$$U_Z(\mathbf{z}) = U_X(\mathbf{x}) + U_Y(\mathbf{y}) + \rho_{inter} U_{XY}(\mathbf{x}, \mathbf{y}).$$

The interaction term U_{XY} involves attractive interactions between segments and rectangles like those presented in figure 7. The goal is to make the information given by rectangles and segments complete

each other, by favoring configurations where segment and rectangle dispositions are consistent. The final energy term involves a set of

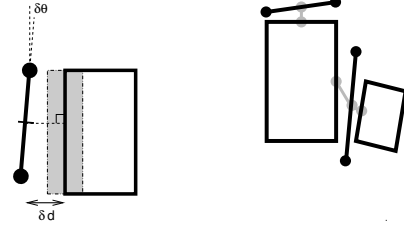


Fig. 7. Attractive interactions between segments and rectangles.

real parameters that allows tuning the influence of each interaction. The probability density function actually belongs to a general exponential family, see [5] for details.

6. ALGORITHM

A simulated annealing is performed on the density of the defined point process Z . The simulated annealing allows to find the configuration of segments and rectangles minimizing the energy. We use a RJMCMC (Reversible Jump Markov Chain Monte Carlo) sampler, derived from the work of C. Geyer and J. Møller in [9] and P.J. Green in [10]. The algorithm is detailed in [4, 5, 7].

6.1. Algorithm

We consider a point process \mathbf{Z} defined by its energy $U(\cdot)$. Through the Gibbs relation, this energy defines a density h known up to a normalizing constant which, together with the distribution $\mu(\cdot)$ of the reference Poisson point process defines the distribution $\pi(\cdot)$ of \mathbf{Z} . A Markov chain $(X_t)_{t \geq 0}$ is defined by a starting point $X_0 = \{\emptyset\}$ and a Markovian transition kernel $P(\mathbf{z}, \cdot)$ which is designed in order to make the Markov Chain converge towards the desired distribution, i.e. such that $\|P^n(\{\emptyset\}, \cdot) - \pi(\cdot)\|_{TV} \rightarrow 0$ where $\|\cdot\|_{TV}$ denotes the Total Variation norm (TV). The algorithm is based on a mixture of perturbation kernels $Q(\cdot, \cdot) = \sum_m p_m Q_m(\cdot, \cdot)$ where $\sum p_m = 1$ and $\int Q_m(\mathbf{z}, \mathbf{z}') \mu(d\mathbf{z}') = 1$. The algorithm iterates the following steps, if the current state X_t is $X_t = \mathbf{z} = \{z_1, \dots, z_n\}$:

1. Choose one of the proposition kernels $Q_m(\cdot, \cdot)$ with probability $p_m(\mathbf{z})$ and sample \mathbf{z}' according to the chosen kernel $\mathbf{z}' \sim Q_m(\mathbf{z}, \cdot)$.
2. Compute the Green ratio $R_m(\mathbf{z}, \mathbf{z}')$, function of the selected kernel Q_m , the original state \mathbf{z} and the proposed new state \mathbf{z}' . The ratio R_m is derived to make the Markov chain converge towards the desired distribution.
3. The proposition is accepted $X_{t+1} = \mathbf{z}'$ with a probability $\alpha_m(\mathbf{z}, \mathbf{z}') = \min(R_m(\mathbf{z}, \mathbf{z}'), 1)$ and rejected otherwise $X_{t+1} = \mathbf{z}$.

6.2. Perturbation kernels

The efficiency of the algorithm highly depends on the variety of possible transformations $Q_m(\mathbf{z}, \cdot)$. We use different types of moves, including *birth or death* of an object, *translation*, *rotation*, *dilation* of a randomly selected object, as well as transformations acting on interaction pairs of objects (see [5] for details). With each of these transformations is associated a Green ratio R_m that insures the convergence of the Markov Chain towards the desired distribution.

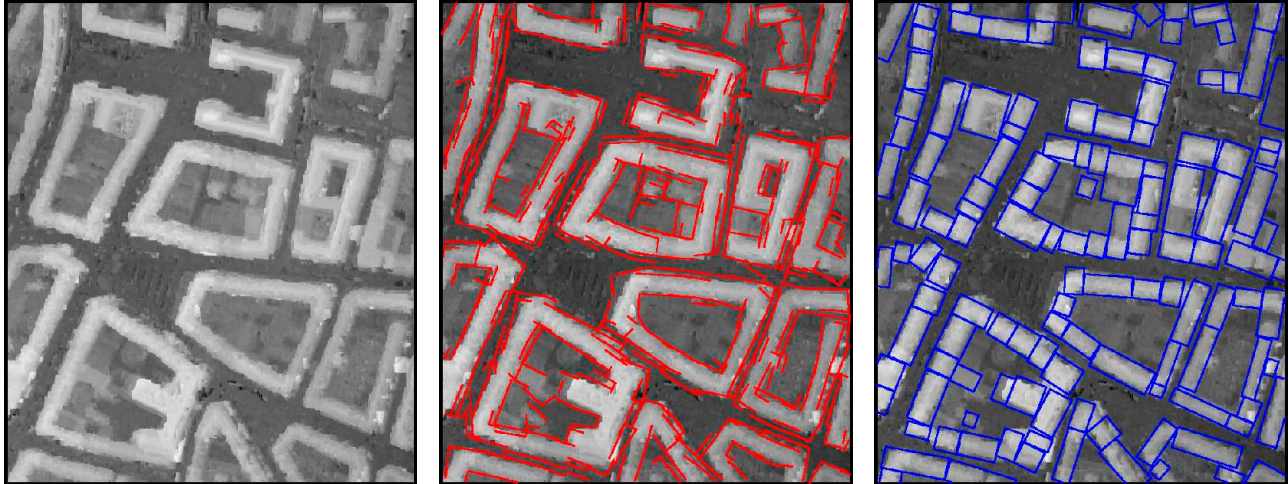


Fig. 8. Results on real data. From left to right: original DEM of the French town of Amiens provided by the French Geographic Institute (©IGN), segment extraction and rectangle extraction results. Additional results are described in [5].

6.3. Simulated annealing

To find a minimizer of the energy $U(\cdot)$ we use a simulated annealing framework. Instead of generating samples of $h(\cdot)$, we simulate $h^{\frac{1}{T_t}}(\cdot)$. The temperature parameter T_t tends to zero as t tends to ∞ . This technique has been widely used in image processing (see [11] for instance). If T_t decreases with a logarithmic rate, then X_t tends to one of the global maximizers of $h(\cdot)$. Of course, in practice it is not possible to use a logarithmic cooling schedule and we eventually use a geometrical one. This last point makes the quality of the proposition kernels an important issue.

7. RESULTS

Figure 8 presents a result on real data obtained in 6 hours for an image of size 1000 by 1000, using using a 3 Ghz Pentium 4 machine. Additional results on different types of data and an extended area can be found in [5], showing that the approach is powerful on data of various kinds.

8. CONCLUSION

This work extends our previous work on the use of stochastic geometry for image feature extraction. We show that combining different objects is powerful and allows dealing with complex real data.

Future work should involve the introduction of more primitives (e.g. corners, roof edges, etc...). However two major issues need to be solved in order to fully exploit this kind of models. First, the learning of parameters should be carefully examined, even if the prior model parameters proved to be very robust in practice. Second, the algorithm employed is very slow. There is a huge need for proposing new algorithms to speed up the computation.

9. REFERENCES

- [1] H.G. Maas and G. Vosselman, "Two algorithms for extracting building models from raw laser altimetry data," *JPRS*, vol. 54, no. 2-3, pp. 153–163, 1999.
- [2] C. Vestri and C. Devernay, "Using robust methods for automatic extraction of buildings," in *CVPR*, 2001.
- [3] S. Vinson, L. D. Cohen, and F. Perlant, "Extraction of rectangular buildings using DEM and orthoimage," in *SCIA*, Bergen, Norway, June 2001.
- [4] M. Ortner, X. Descombes, and J. Zerubia, "Building outline extraction from Digital Elevation Models using marked point processes," *International Journal of Computer Vision*, 2005, To appear.
- [5] M. Ortner, X. Descombes, and J. Zerubia, "A marked point process of rectangles and segments for automatic analysis of Digital Elevation Models.," *INRIA Research Report 5712*, October 2005.
- [6] A. Baddeley and M. N. M. Van Lieshout, "Stochastic geometry models in high-level vision," *Statistics and Images*, vol. 1, pp. 233–258, 1993.
- [7] M. Ortner, X. Descombes, and J. Zerubia, "A Reversible Jump MCMC sampler for building detection in image processing.," in *Monte Carlo methods and quasi-Monte Carlo methods*, Juan les Pins (France), June 2004, To appear in LNS, Springer Verlag.
- [8] M. N. M. Van Lieshout, "Stochastic annealing for nearest-neighbour point processes with application to object recognition.," *CWI Research Report, BS-R9306, ISSN 0924-0659*, 1993.
- [9] C.J. Geyer and J. Møller, "Simulation and likelihood inference for spatial point processes," *Scandinavian Journal of Statistics*, vol. Series B, 21, pp. 359–373, 1994.
- [10] P.J. Green, "Reversible jump Markov chain Monte-Carlo computation and Bayesian model determination," *Biometrika*, vol. 57, pp. 97–109, 1995.
- [11] G. Winkler, *Image Analysis, Random Fields and Markov Chain Monte Carlo Methods: a Mathematical Introduction*, Springer-Verlag, 2003, Second Edition.